SUPPLEMENTAL DATA

Proteostasis Regulators and Pharmacologic Chaperones Synergize to Correct Protein Misfolding Diseases

Ting-Wei Mu,[1,4] Derrick Sek Tong Ong,[1,4] Ya-Juan Wang,[1,2]

William E. Balch,[3] John R. Yates,[2] Laura Segatori,[1,4,5,*] and Jeffery W. Kelly[1,*]

[1]Department of Chemistry and The Skaggs Institute for Chemical Biology, [2]Department of Chemical Physiology, [3]Department of Cell Biology, The Scripps Research Institute, La Jolla, CA 92037

[4]These authors contributed equally to this work.

[5]Current Address: Department of Chemical and Biomolecular Engineering, Rice University, 6100 Main Street, MS-362, Houston, TX 77005

[*]To whom correspondence should be addressed.

E-mail: jkelly@scripps.edu, segatori@rice.edu

Supplemental Discussion

We considered the possibility that the low levels of celastrol and MG-132 employed in this study may have resulted in a preconditioning phenomenon (Lu et al., 2004), whereby the mild ER stress imposed by these small molecules activates all the UPR sensors to facilitate protein folding and adaptation (Rutkowski et al., 2006). However, low levels of thapsigargin (ranging from 0.001 to 100 nM), an ER stressor, did not enhance L444P GC folding, trafficking or lysosomal activity (data not shown), suggesting that preconditioning is an unlikely explanation for PR function.

Supplemental Experimental Procedures

Reagents. Celastrol, MG-132, PS I, PS IV, Tyropeptin A, and lactacystin were from Calbiochem (San Diego, CA). N-(n-nonyl)deoxynojirimycin (NN-DNJ), 2-acetamido-2-deoxynojirimycin (ADNJ), 4-methylumbelliferyl 6-sulfo-2-acetamido-2-deoxy-β-D-glucopyranoside (MUGS), Conduritol B Epoxide (CBE) were from Toronto Research Chemicals (Downsview, ON, Canada). 4-methylumbelliferyl β-D-glucoside (MUG) was from Sigma (St. Louis, MO). Cell culture media were purchased from Gibco (Grand Island, NY).

Cell cultures. Primary skin fibroblast cultures were established from patients homozygous for the G202R (c.721G>A) and the N370S (c.1226A>G) mutations. Wild type primary skin fibroblasts (GM05659, GM00498), the Gaucher disease fibroblast cell line homozygous for the L444P (c.1448T>C) mutation (GM08760), and the Tay-Sachs disease fibroblast cell line heterozygous for the G269S (c.805G>A) mutation and a 4 base pair insertion (c.1278insTATC) (GM13204) were obtained from Coriell Cell Repositories (Camden, NJ). Fibroblasts were grown in minimal essential medium with Earle's salts supplemented with 10% heat-inactivated fetal bovine serum and 1% glutamine Pen-Strep at 37°C in 5% CO_2. Cell medium was replaced every 3 or 4 days. Monolayers were passaged upon reaching confluency with TrypLE Express.

Enzyme activity assays. The intact cell GC activity assay has been previously described (Sawkar et al., 2002). Briefly, approximately 10^4 cells were plated in each well of a 96-well plate (100 μl per well) overnight to allow cell attachment. Medium was replaced with fresh medium containing small molecules and plates were incubated at 37°C. Trypan blue staining was utilized to measure cell viability after drug treatment. The medium was then removed and monolayers washed with PBS. The assay reaction was started by the addition of 50 μl of 2.5mM MUG in 0.2 M acetate buffer (pH 4.0) to each well. Plates were incubated at 37°C for 7 hours and the reaction was stopped by the addition of 150 μl of 0.2 M glycine

buffer (pH 10.8) to each well. Liberated 4-methylumbelliferone was measured (excitation 365 nm, emission 445 nm) with a SpectraMax Gemini plate reader (Molecular Device, Sunnyvale, CA). Control experiments to evaluate the extent of unspecific non-lysosomal GC activity were performed by adding CBE to the assay reaction. Typically, culture medium was replaced with medium containing small molecule after overnight incubation (time 0). Alternatively, when L444P GC fibroblasts were incubated with celastrol or with NN-DNJ and celastrol, after adding the compounds at time 0, the medium was replaced every 24 hours (or as indicated in the Results and Figures for each specific experiment) with fresh medium containing the same compound concentration that was originally present in each well, as described in the Results section. GC activities measured were normalized to the corresponding protein concentration for each sample.

The Hex α-site cell assay has been previously described (Tropak et al., 2004). Cells were plated as described for the GC assay. After 1 to 8 days of incubation the medium was removed, cells were washed with PBS, and lysed with 60 µl of 10 mM citrate/phosphate buffer pH 4.2 (CP buffer) containing 0.5% human serum albumin and 0.5% Triton X-100. 30 µl of aliquots were transferred to a 96-well plate and Hex α-site activity was measured by adding 30 µl of 3.2 mM MUGS in CP buffer to each well and incubating the plates at 37°C for 1 to 7 hour. The reaction was stopped by adding 200 µl of 0.1 M 2-amino-2-methyl-1-propanol (pH 10.5) and the fluorescence was measured (excitation 365 nm, emission 450 nm).

For both the Hex α-site and the GC activity assays each data point reported was evaluated at least in triplicate in each plate, and on three different days. The data reported were normalized to the activity of untreated cells, and expressed as the percentage of WT enzyme activity for each different cell line. The data were reported as mean ± SEM.

Western blot analysis. Cells were lysed with the complete lysis-M buffer containing complete protease inhibitor cocktail (Roche, Nutley, NJ). Total cell protein was determined with Micro BCA assay reagent (Pierce, Rockford, IL) and each sample was diluted to the same protein concentration. Company specifications were followed for protein treatment with Endo H and PNGase F (New England Biolabs, Ipswich, MA). Aliquots of cell lysates were separated in a 10% SDS-PAGE gel and Western blot analysis was performed using appropriate antibodies. Rabbit anti-Hsp40, anti-Hsp70, anti-HSF1, anti-calnexin, anti-ubiquitin, and anti-actin, as well as mouse anti-Hsp90, anti-Hsp27, anti-αB crystallin and anti-calreticulin were from Stressgen (Victoria, BC, Canada). Mouse monoclonal anti-GC 2E2 was from Novus Biologicals (Littleton, CO). Rabbit anti-BiP, anti-GRP94, and anti-IRE1α were from Santa Cruz Biotechnology. Mouse monoclonal anti-ATF6 was from IMGENEX (San Diego, CA). Secondary goat anti-rabbit and goat anti-mouse HRP-conjugated antibodies were from Pierce. Blots were visualized using SuperSignal West Femto Maximum Sensitivity or West Pico Substrate (Pierce). The Western blot bands of the endoH treated samples were quantified by Java Image processing and analysis software from the NIH (http://rsb.info.nih.gov/ij/).

Cell-based chymotrypsin-like proteasomal activity assay. Proteasome-Glo Cell-Based Assay kit (Promega, Madison, WI) was utilized to measure the chymotrypin-like proteasomal activity. Briefly, approximately $5x10^3$ L444P GC cells were plated in each well of a 96-well plate (100 μl per well) overnight to allow cell attachment. Medium was replaced with fresh medium containing proteasome inhibitors at various concentrations. After 2 h incubation at 37°C, following the company's instruction, 100 μl/well of Proteasome-Glo Cell-Based reagent was added and luminescence measured with a SpectraMax Gemini plate reader. The luminescence of treated cells was normalized to that of untreated cells after background subtraction. IC_{50} values were calculated by fitting the data to the formula: $y = IC_{50} / (IC_{50} + x)$, where y is the normalized luminescence signal, and x is the inhibitor concentration. Each data

point was evaluated at least in triplicate, and on three different days. The data are reported as IC_{50} ± SD in the text. A similar protocol was used to determine the proteasome activity after the treatment with 0.25 μM MG-132 or 0.8 μM celastrol for 1 d and 3d. The percentage proteasome inhibition was normalized to the proteasome activity measured after DMSO treatment.

Relative quantification of protein expression level changes by Multidimensional Protein Identification Technology (MudPIT). Proteins from each sample were precipitated using 25% trichloroacetic acid (v/v) and ice-cold acetone. The pellet was air-dried and suspended with 8 M urea containing 1× Invitrosol (Invitrogen, Calsbad, CA) in 100 mM Tris-HCl pH 8.5. The protein concentration was measured using the BCA Protein Assay Kit (Pierce). An amount of 200 μg of total protein was first reduced by incubating with Tris(2-carboxyethyl) phosphine (TCEP) at 5 mM for 30 min, and then alkylated by incubating with iodoacetamide (IAA) at 10 mM for 20 min in the dark. The samples were subsequently diluted to 2 M urea with 100 mM Tris-HCl, pH 8.5, brought to 1 mM $CaCl_2$, and digested by adding sequence grade modified trypsin (Promega, Madison, WI) at an enzyme/substrate ratio of 1:30 and incubating overnight at 37°C. The digestion reaction was quenched by adding formic acid to 5% (v/v) to lower the pH to 2-3. Samples not immediately analyzed were stored at -80°C.

For each sample, three replicates of 60 μg of the protein digest were analyzed each time by MudPIT (Link et al., 1999; Washburn et al., 2001). Peptide mixture was pressure-loaded onto a 250-μm i.d. fused silica capillary column packed with 2.5 cm Partisphere strong cation exchanger (Whatman, Clifton, NJ) and 2.5 cm 5-μm Aqua C18 material (Phenomenex, Ventura, CA). The column was washed for 30 min with buffer containing 95% water, 5% acetonitrile (ACN), and 0.1% formic acid. After desalting, it was attached to a 100-μm i.d. capillary with a 5-μm pulled tip packed with 12 cm 5-μm Aqua C18 material, and the entire column was placed inline with an Agilent 1100 quaternary HPLC (Agilent, Palo Alto, CA). The sample was analyzed using a fully automated 12-step separation procedure. The buffer solutions used

for the chromatography were 5% ACN/0.1% FA (buffer A), 80% ACN/0.1% FA (buffer B), and 500 mM ammonium acetate/0.1% FA (buffer C). The first step consisted of a 100 min gradient from 0 to 100% buffer B. Steps 2-11 had the following profile: 3 min of 100% buffer A, 3 min of *X*% buffer C, a 10 min gradient from 0 to 15% buffer B, and a 97 min gradient from 15 to 55% buffer B. The 3 min buffer C percentages (*X*) were 5, 10, 20, 30, 40, 50, 60, 70, 80 and 90%, respectively. In the final step, the gradient contained: 3 min of 100% buffer A, 10 min of 100% buffer C, a 10 min gradient from 0 to 15% buffer B, and a 107 min gradient from 15 to 100% buffer B. As peptides were being eluted from the microcapillary column, they were electrosprayed directly into a linear LTQ ion trap mass spectrometer (ThermoFinnigan, San Jose, CA) with the application of a 2.4 kV spray voltage. A cycle of one full scan mass spectrum (400-1400 m/z) followed by 5 data-dependent MS/MS spectra, at a 35% normalized collision energy and with dynamic exclusion enabled, was repeated continuously throughout each step of the multidimensional separation.

Acquired tandem mass spectra were searched against the European Bioinformatics Institute International Protein Index human protein database (version 3.30, released on June 28, 2007). In order to calculate confidence levels and false positive rates, a decoy database containing the reverse sequences was appended to the target database, and the SEQUEST (Eng et al., 1994) algorithm was used to find the best matching sequences from the combined database. SEQUEST results were assembled and filtered by DTASelect (Tabb et al., 2002). At least two peptides per protein and a false positive rate of less than 1% at the protein level were required.

Estimation of protein abundance based on spectra count was used as the relative quantification method (Liu et al., 2004) which has been widely applied (Cao et al., 2008; Liao et al., 2007; Rikova et al., 2007). Spectra counts from the three replicates of each sample were merged to average the run to run variation. Although the total number of spectra was similar between any two samples, a normalization factor (F =

Total number of spectra in control sample/Total number of spectra in treated sample) was applied, that is, the spectra count ratio of the treated sample versus the control sample multiplied by the normalization factor gives the normalized ratio. If a protein is detected in both untreated and treated samples, proteins with expression level changes were filtered according to the following criteria: (1) if the same protein was identified in both samples with spectra counts greater than 10, normalized spectra count ratios of 2 or above were considered as increased, likewise, 0.5 or less as decreased; (2) if the same protein was identified in both samples with a spectra count from either of them less than 10 but the difference between the two was great than 10, normalized spectra count ratios of 2.5 or above were considered as increased, likewise, 0.4 or less as decreased. If a protein was identified in only one sample, a spectra count of greater than 20 was used to consider a significant change; a preliminary analysis of this category showed that treatment of L444P GC fibroblast with MG-132 (0.8 μM) for 3 d upregulated 83 proteins and down regulated 85 proteins, while treatment of L444P GC fibroblast with celastrol (0.8 μM) for 3 d upregulated 106 proteins and down regulated 87 proteins, amongst the 1000 proteins detected in this category, indicating that the PR treatment modestly affect the proteome globally along with the data shown in Figure 2A, where a protein is detected in both untreated and treated samples.

Quantitative RT-PCR. The cells were incubated with drugs at 37 °C for the indicated amount of time before total RNA was extracted from the cells using RNeasy Mini Kit (Qiagen #74104). cDNA was synthesized from 500 ng of total RNA using QuantiTect Reverse Transcription Kit (Qiagen #205311). Quantitative PCR reactions were performed using cDNA, QuantiTect SYBR Green PCR Kit (Qiagen #204143) and corresponding primers in the ABI PRISM 7900 system (Applied Biosystems). The forward and reverse primers for Hsp40, Hsp70, Hsp90, Hsp27, αB-crystallin (CRYAB), BiP, GRP94, calnexin (CNX), calreticulin (CRT), CHOP, ATF6, PERK, and HSF1, and endogenous housekeeping gene, GAPDH, are listed in Table S1. Samples were heated for 15 min at 95°C and amplified in 45 cycles of 15

s at 94°C, 30 s at 57°C, and 30 s at 72°C. Analysis was done using SDS2.1 software (Applied Biosystems). Threshold cycle (C_T) was extracted from the PCR amplification plot. The ΔC_T value was used to describe the difference between the C_T of a target gene and the C_T of the housekeeping gene: ΔC_T = C_T (target gene) - C_T (housekeeping gene). The relative mRNA expression level of a target gene of drug-treated cells was normalized to that of untreated cells: Relative mRNA expression level = 2 exp [-(ΔC_T (treated cells) - ΔC_T (untreated cells))]. Each data point was evaluated in triplicate, and measured three times.

RT-PCR analysis of Xbp-1 splicing. cDNA was synthesized as in quantitative RT-PCR. PCR reactions were performed using cDNA, Taq DNA polymerase (Roche) and corresponding primers listed in Table S1. Samples were heated for 5 min at 95°C, amplified in 30 cycles of 60 s at 95°C, 30 s at 58°C, and 30 s at 72°C, and 5 min at 72°C. PCR products were separated on a 2.5% agarose gel. Unspliced Xbp-1 yielded a 289 bp amplicon, and spliced Xbp-1 yielded a 263 bp amplicon. The experiments were performed three times and similar results were obtained.

Determination of folding and export of ΔF508 CFTR from the ER. CFBE41o- cell lines expressing ΔF508 CFTR were untreated, treated with MG-132 or celastrol for 24 h before being lysed for SDS-PAGE and Western blot analysis. The steady-state pool of band B (ER glycoform) and band C (post-Golgi glycoform) was determined using the antibody against CFTR (M3A7), as described in (Wang et al., 2006).

Supplemental References

Cao, R., He, Q.Y., Zhou, J., He, Q.Z., Liu, Z., Wang, X.C., Chen, P., Xie, J.Y., and Liang, S.P. (2008). High-throughput analysis of rat liver plasma membrane proteome by a nonelectrophoretic in-gel tryptic digestion coupled with mass spectrometry identification. J Proteome Res *7*, 535-545.

Eng, J.K., McCormack, A.L., and Yates, J.R. (1994). An approach to correlate tandem mass-spectral data of peptides with amino-acid-sequences in a protein database. J Am Soc Mass Spectrom *5*, 976-989.

Liao, L., Pilotte, J., Xu, T., Wong, C.C.L., Edelman, G.M., Vanderklish, P., and Yates, J.R. (2007). BDNF induces widespread changes in synaptic protein content and up-regulates components of the translation machinery: An analysis using high-throughput proteomics. J Proteome Res *6*, 1059-1071.

Link, A.J., Eng, J., Schieltz, D.M., Carmack, E., Mize, G.J., Morris, D.R., Garvik, B.M., and Yates, J.R. (1999). Direct analysis of protein complexes using mass spectrometry. Nat Biotechnol *17*, 676-682.

Liu, H.B., Sadygov, R.G., and Yates, J.R. (2004). A model for random sampling and estimation of relative protein abundance in shotgun proteomics. Anal Chem *76*, 4193-4201.

Lu, P.D., Jousse, C., Marciniak, S.J., Zhang, Y.H., Novoa, I., Scheuner, D., Kaufman, R.J., Ron, D., and Harding, H.P. (2004). Cytoprotection by pre-emptive conditional phosphorylation of translation initiation factor 2. EMBO J *23*, 169-179.

Rikova, K., Guo, A., Zeng, Q., Possemato, A., Yu, J., Haack, H., Nardone, J., Lee, K., Reeves, C., Li, Y., *et al.* (2007). Global survey of phosphotyrosine signaling identifies oncogenic kinases in lung cancer. Cell *131*, 1190-1203.

Rutkowski, D.T., Arnold, S.M., Miller, C.N., Wu, J., Li, J., Gunnison, K.M., Mori, K., Akha, A.A.S., Raden, D., and Kaufman, R.J. (2006). Adaptation to ER stress is mediated by differential stabilities of pro-survival and pro-apoptotic mRNAs and proteins. PLoS Biol *4*, 2024-2041.

Sawkar, A.R., Adamski-Werner, S.L., Cheng, W.C., Wong, C.H., Beutler, E., Zimmer, K.P., and Kelly, J.W. (2005). Gaucher disease-associated glucocerebrosidases show mutation-dependent chemical chaperoning profiles. Chem Biol *12*, 1235-1244.

Sawkar, A.R., Cheng, W.C., Beutler, E., Wong, C.H., Balch, W.E., and Kelly, J.W. (2002). Chemical chaperones increase the cellular activity of N370S beta-glucosidase: a therapeutic strategy for Gaucher disease. Proc Natl Acad Sci U S A *99*, 15428-15433.

Tabb, D.L., McDonald, W.H., and Yates, J.R. (2002). DTASelect and contrast: Tools for assembling and comparing protein identifications from shotgun proteomics. J Proteome Res *1*, 21-26.

Tropak, M.B., Reid, S.P., Guiral, M., Withers, S.G., and Mahuran, D. (2004). Pharmacological enhancement of beta-hexosaminidase activity in fibroblasts from adult Tay-Sachs and Sandhoff Patients. J Biol Chem *279*, 13478-13487.

Wang, X.D., Venable, J., LaPointe, P., Hutt, D.M., Koulov, A.V., Coppinger, J., Gurkan, C., Kellner, W., Matteson, J., Plutner, H., *et al.* (2006). Hsp90 cochaperone Aha1 downregulation rescues misfolding of CFTR in cystic fibrosis. Cell *127*, 803-815.

Washburn, M.P., Wolters, D., and Yates, J.R. (2001). Large-scale analysis of the yeast proteome by multidimensional protein identification technology. Nat Biotechnol *19*, 242-247.

Supplemental Figure Legends

Figure S1. Western blot analysis of GC trafficking in L444P GC fibroblasts. L444P GC fibroblasts were treated for 72 h with 0.25 μM MG-132 (**M**) or 0.8 μM celastrol (**C**). Untreated WT and L444P cells served as positive and negative controls, respectively. Equal amount of total proteins from lysed cells were digested with buffer only, Endo H, or PNGase F before separation in a 10% SDS-PAGE gel and detection using mouse anti-GC antibody 2E2. Endo H resistant GC bands reflect the mature lysosomally localized glycoform of GC. PNGase F digestion yielded the deglycosylated GC form. The gel images were taken from the same blot but with different exposure times because longer exposure is required to visualize the EndoH resistant bands. β-actin serves as a loading control.

Figure S2. Optimization of celastrol dosing regime in L444P GC fibroblasts. Activities were normalized to the activity of untreated L444P GC cells (left y axis) and expressed as the percentage of WT GC activity (right y axis). The data were reported as mean ± SEM. **A**) L444P GC activity within fibroblasts treated with celastrol for 120 h at medium concentrations ranging from 0.1 to 1.2 μM. The blue curve indicates administration of celastrol at t=0, with no media or celastrol changes thereafter, while the red curve results from celastrol administration at t=0, 24, 48, 72, and 96 h, enabled by media changes. **B**) Relative GC activity of L444P GC fibroblasts exposed to celastrol at time 0, thereafter the media was replaced at 72 h with celastrol free media, and L444P GC activity was measured at 72, 96, 120, 144, 168 and 192 h. The celastrol-mediated L444P GC activity is sustained for 96 h after a single dose. **C**) Relative GC activity of L444P GC fibroblasts exposed to celastrol at t=0, 24 and 48 h and the media was replaced by celastrol free media at 72 h and L444P GC activity was measured at 72, 96, 120, 144, 168 and 192 h. This exhibited retention of activity for 120 h.

Figure S3. Effect of MG-132 and celastrol on the activity of other WT lysosomal enzymes in L444P fibroblasts, as well as GC in WT GC fibroblasts (indicated by asterisk). After incubation with 0.8 μM MG-132 or 0.8 μM celastrol for 24 h, L444P GC fibroblasts were assayed for the activities of α-mannosidase, α-glucosidase, β-glucuronidase, α-galactosidase, β-galactosidase, heparan sulfate sulfamidase (SGSH), and α-N-acetylglucosaminidase (NAGLU), and WT GC fibroblasts were assayed for the GC activity, with their corresponding substrates using a lysed cell enzyme activity assay, as previously described (Sawkar et al., 2005). The enzyme activity of treated cells was normalized against that of untreated cells of the same type. Each data point was evaluated at least in triplicate in each plate, and on three different days. The data were reported as mean ± SEM.

Figure S4. Effect of proteasome inhibitors on GC activity in L444P GC fibroblasts. L444P GC fibroblasts were exposed to a variety of proteasome inhibitors including MG-132, PS I, PS IV, and Tyropeptin A for 96 h (**A**), and lactacystin for 24 h (**B**) without a media change before the GC activities were measured. The enzyme activity of treated cells was reported relative to the activity of untreated cells of the same type (left y axis) and as the percentage of WT GC activity (right y axis). The data were expressed as mean ± SEM.

Figure S5. Knockdown and inactivation of IRE1α signaling by siRNA. L444P GC cells were treated with non-targeting or corresponding siRNA, or mock transfected for 24 h, and DMSO, or 0.8 μM celastrol for another 24 h before being lysed for RNA extraction and probed by RT-PCR analysis for Xbp-1 splicing, as in Figure 4A. L444P GC cells treated with 10 μg/ml tunicamycin for 6 h were also probed as a positive control, and GAPDH was used as a housekeeping control. Efficient IRE1α knockdown was confirmed by the dramatically decreased Xbp1 splicing in the presence of 0.8 μM celastrol in IRE1α knockdown cells (cf. lanes 8, 9, and 11).

Figure S6. A GC pharmacologic chaperone, NN-DNJ, does not induce the heat shock response and the unfolded protein response in N370S and L444P GC cells. Relative chaperone mRNA expression levels probed by quantitative RT-PCR in N370S GC fibroblasts (**A**) and in L444P GC fibroblasts (**B**) after the treatment with 5 μM NN-DNJ for 24 h and 120 h. Relative mRNA expression level for treated GC cells was normalized to that of untreated cells of the same cell type after correction to the expression level of GAPDH, a housekeeping control. The data in (**A**) and (**B**) were reported as mean ± SEM. **C**) Detection of spliced Xbp-1 mRNA by RT-PCR in N370S or L444P GC fibroblasts after the treatment with 5 μM NN-DNJ for 1 d and 5 d. L444P GC cells treated with 10 μg/ml tunicamycin for 6 h were also probed as a positive control and GAPDH was used as a housekeeping control. Xbp1-u represents unspliced Xbp-1, a 289 bp amplicon, and Xbp1-s represents spliced Xbp-1, a 263 bp amplicon.

Figure S7. 2D plots showing GC activity of G202R and N370S GC patient derived fibroblasts cultured with media containing celastrol and NN-DNJ. The data were reported as mean ± SEM. **A**) Relative GC activity of G202R GC fibroblast cell lines. Four sets of cultures were prepared and incubated with celastrol at 0, 0.4, 0.6 or 0.8 μM. Each set was additionally supplemented with NN-DNJ at medium concentration ranging from 1 to 20 μM. GC activities were measured after 4 days of growth and normalized to the GC activity of untreated cells. **B**) Relative GC activity of G202R GC fibroblast cell lines. Four sets of cultures were prepared and incubated with NN-DNJ at 0, 2, 5 or 20 μM. Each set was additionally supplemented with celastrol at medium concentration ranging from 0.2 to 1.2 μM. GC activities were measured after 4 days of growth and normalized to the GC activity of untreated cells. **C**) Relative GC activity of N370S GC fibroblast cell lines. Cells were grown and treated, and GC activities measured as described in **A**. **D**) Relative GC activity of N370S GC fibroblast cell lines. Cells were grown and treated, and GC activities measured as described in **B**.

Figure S8. Cells were plated and treated according to the experimental design described in Figure S7 with the exception that the incubation medium was replaced at t= 0, 30, 60, 72, 102, and 132 h. Media was supplemented with celastrol at t=0, 30, 72, and 102 h, while it was supplemented with both celastrol and NN-DNJ at t= 60 and 132 h (see also the schematic on the bottom of Figure 6C). L444P GC activity was measured after 144 h and normalized to the activity of untreated cells. The data were reported as mean ± SEM. **A**) Relative GC activity of L444P GC fibroblasts incubated with media concentration of NN-DNJ ranging from 0.25 to 5 μM and a constant concentration of celastrol of 0, 0.1, 0.2, 0.4, or 0.6 μM. **B**) Relative GC activity of L444P GC fibroblasts incubated with medium concentration of celastrol ranging from 0.2 to 1.2 μM and a constant concentration of NN-DNJ of 0, 0.5, 1, 2, or 4 μM.

Figure S9. Relative L444P GC activity in patient-derived fibroblasts cultured with media containing MG-132 and NN-DNJ. The media was replaced at multiple times according to the same procedures described for celastrol and NN-DNJ in Figure S8 and represented in the schematic of Figure 6D. Relative L444P GC activity was measured after 144 h and normalized to the activity of untreated cells of the same type. The data were reported as mean ± SEM. **A**) Relative GC activity of L444P GC fibroblasts incubated with medium concentrations of NN-DNJ ranging from 0.25 to 5 μM and a constant concentration of MG-132 of 0, 0.2, 0.4, 0.6, or 0.8 μM. **B**) Relative GC activity of L444P GC fibroblasts incubated with medium concentrations of MG-132 ranging from 0.2 to 1.2 μM and a constant concentration of NN-DNJ of 0, 0.5, 1, 5, or 10 μM.

Figure S10. Relative Hex α-site activity in αG269S/1278insTATC HexA Tay-Sachs fibroblast cell line cultured with media containing celastrol, ADNJ (an enzyme-specific pharmacologic chaperone), or MG-132 and ADNJ. Activities were reported relative to the activity of untreated cells of the same type (left y

axis) and as the percentage of WT Hex α-site activity (right y axis). αG269S/1278insTATC HexA fibroblasts were exposed to **A**) 0.2 to 1.2 μM celastrol and the Hex α-site activities measured at 24, 48, 72, 96, 120 h; **B**) 5 to 100 μM ADNJ and the Hex α-site activities measured at 96, 120, 144, 168, 192 h; **C**) medium containing ADNJ ranging from 2 to 50 μM and a constant concentration of MG-132 of 0, 0.2, 0.4, 0.6, 0.8 or 1.0 μM and Hex α-site activity measured after 6 days; **D**) medium containing MG-132 ranging from 0.2 to 1.2 μM and a constant concentration of ADNJ of 0, 2, 5, 10, 20 or 50 μM and Hex α-site activity measured after 6 days. The data were reported as mean ± SEM.

Figure S11. Effect of celastrol and MG-132 on folding and export of ΔF508 CFTR from the ER. CFBE41o- cell lines expressing ΔF508 CFTR were untreated, treated with MG-132 (**A**) or celastrol (**B**) for 24 h before being lysed for SDS-PAGE and Western blot analysis. Two replicates were probed for CFTR to evaluate the drug effect. The steady-state pool of band B (ER glycoform) and band C (post-Golgi glycoform) was determined as described in (Wang et al., 2006). Actin served as a gel loading control.

Table S1. Primer sequences used in quantitative RT-PCR and RT-PCR

Gene	GenBank Accession Code	Forward Primer	Reverse Primer
GAPDH	NM_002046	5'-GTC GGA GTC AAC GGA TT-3'	5'-AAG CTT CCC GTT CTC AG-3'
Hsp40	NM_006145	5'-CGC CGA GGA GAA GTT C-3'	5'-CAT CAA TGT CCA TGC CTT-3'
Hsp70	NM_005345	5'-GGA GGC GGA GAA GTA CA-3'	5'-GCT GAT GAT GGG GTT ACA-3'
Hsp90	NM_005348	5'-GAT AAA CCC TGA CCA TTC C-3'	5'-AAG ACA GGA GCG CAG TTT CAT AAA-3'
Hsp27	X54079	5'-AAG TTT CCT CCT CCC TGT CC-3'	5'-CGG GCT AAG GCT TTA CTT GG-3'
CRYAB	NM_001885	5'-CAC CCA GCT GGT TTG ACA CT-3'	5'-TGA CAG AGA ACC TGT CCT TCT-3'
BiP	NM_005347	5'-GCC TGT ATT TCT AGA CCT GCC-3'	5'-TTC ATC TTG CCA GCC AGT TG-3'
GRP94	NM_003299	5'-GGC CAG TTT GGT GTC GGT TT-3'	5'-CGT TCC CCG TCC TAG AGT GTT-3'
CNX	NM_001746	5'-GCG TTG TGG GGC AGA TGA T-3'	5'-CCG GTT GAG GTG CAT CAG T-3'
CRT	NM_004343	5'-AAG TTC TAC GGT GAC GAG GAG-3'	5'-GTC GAT GTT CTG CTC ATG TTT C-3'
CHOP	NM_004083	5'-ACC AAG GGA GAA CCA GGA AAC G-3'	5'-TCA CCA TTC GGT CAA TCA GAG C-3'
ATF6	NM_007348	5'-TGC TTC CAG CAG CAC CCA AGA CTC-3'	5'-CCC AGC AAC AGC AAG GAC TGG C-3'
PERK	NM_004836	5'-GAG CTG TCG GAC CTC GCA GTG-3'	5'-GGC AGC TTC CTG TTC TTC CAC ATC TG-3'
HSF1	NM_005526	5'-TCC TGC TGG ACC CCG GCT-3'	5'-CTA GGA GAC AGT GGG GTC CTT-3'
Xbp-1	NM_005080	5'-TTA CGA GAG AAA ACT CAT GGC-3'	5'-GGG TCC AAG TTG TCC AGA ATG C-3'

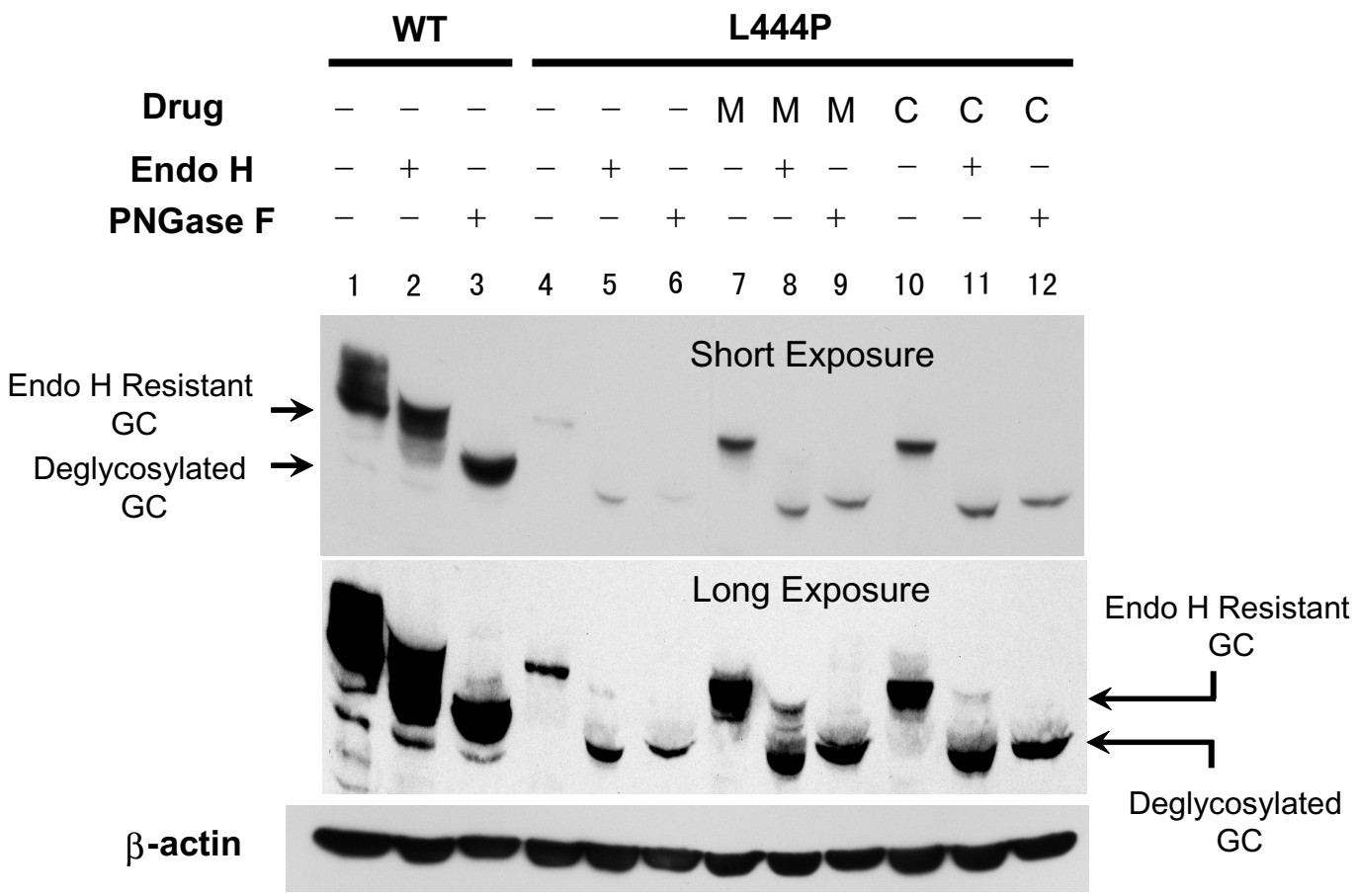
WT
L444P
Drug
Endo H
PNGase F
1 2 3 4 5 6 7 8 9 10 11 12
Short Exposure
Endo H Resistant GC
Deglycosylated GC
Long Exposure
Endo H Resistant GC
Deglycosylated GC
β-actin

Figure S1

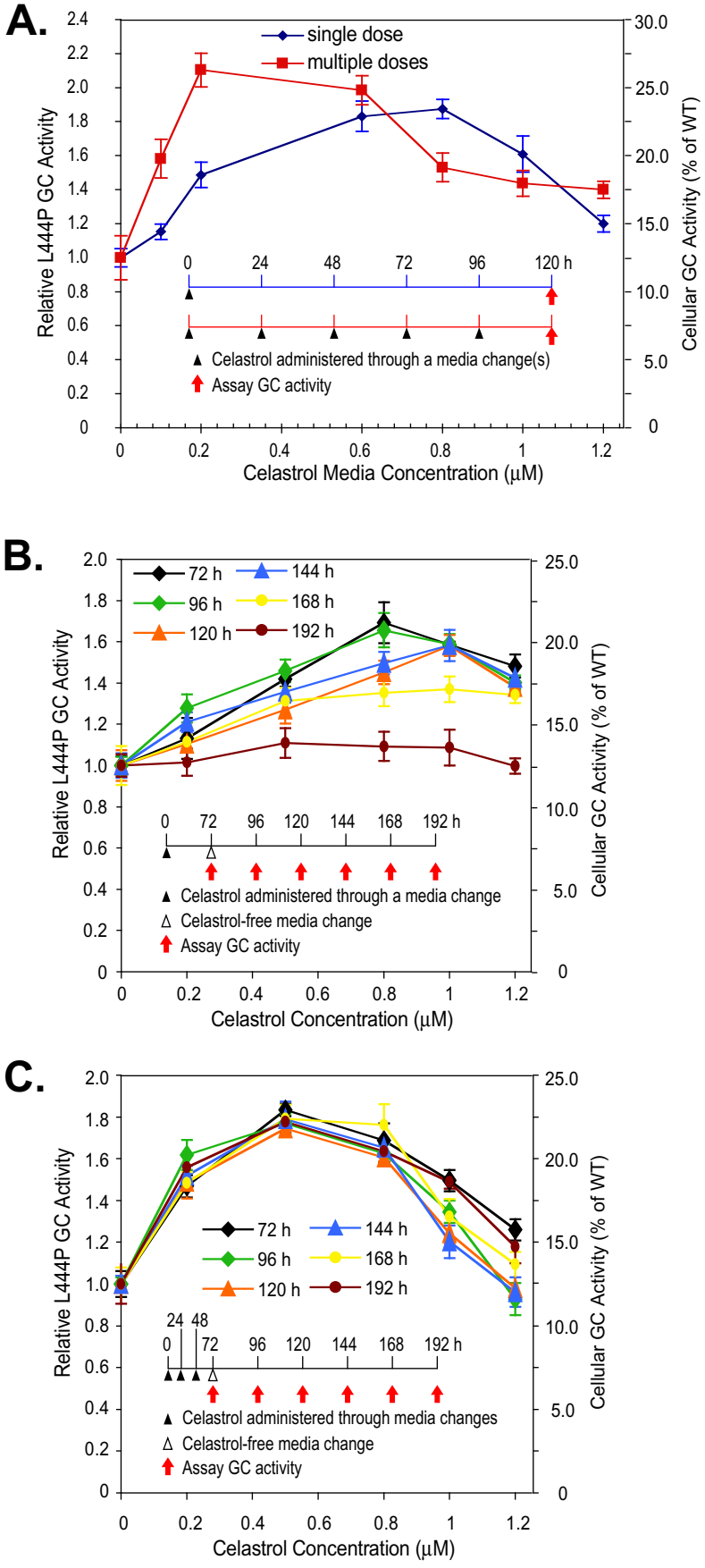
A.
single dose
multiple doses
Relative L444P GC Activity
Cellular GC Activity (% of WT)
Celastrol Media Concentration (μM)
0 24 48 72 96 120 h
Celastrol administered through a media change(s)
Assay GC activity
B.
72 h
96 h
120 h
144 h
168 h
192 h
Relative L444P GC Activity
Cellular GC Activity (% of WT)
Celastrol Concentration (μM)
0 72 96 120 144 168 192 h
Celastrol administered through a media change
Celastrol-free media change
Assay GC activity
C.
72 h
96 h
120 h
144 h
168 h
192 h
Relative L444P GC Activity
Cellular GC Activity (% of WT)
Celastrol Concentration (μM)
24 48
0 72 96 120 144 168 192 h
Celastrol administered through media changes
Celastrol-free media change
Assay GC activity

Figure S2

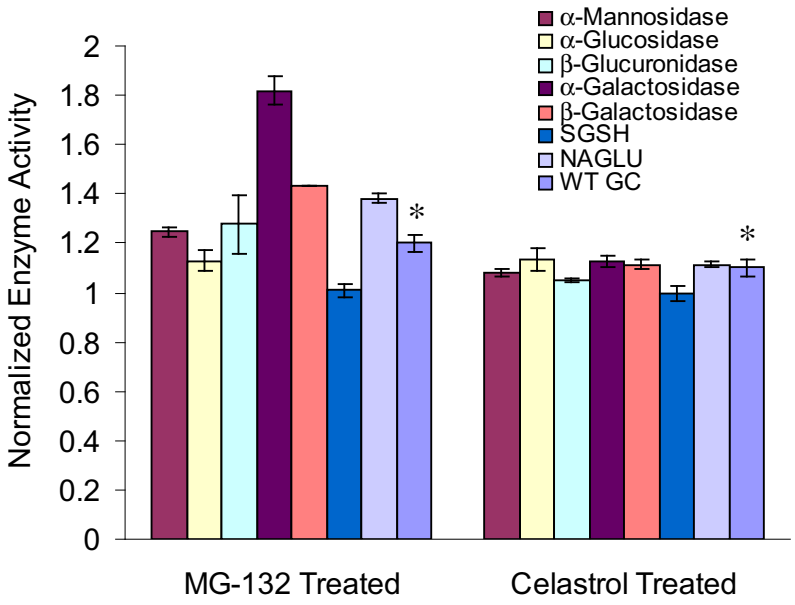
α-Mannosidase
α-Glucosidase
β-Glucuronidase
α-Galactosidase
β-Galactosidase
SGSH
NAGLU
WT GC
Normalized Enzyme Activity
2
1.8
1.6
1.4
1.2
1
0.8
0.6
0.4
0.2
0
*
*
MG-132 Treated
Celastrol Treated

Figure S3

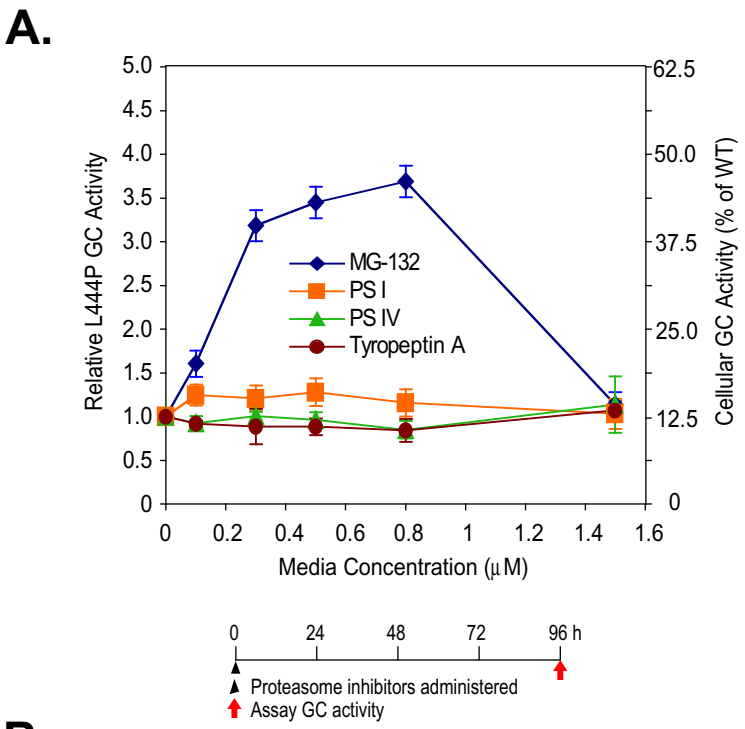
A.
Relative L444P GC Activity
Cellular GC Activity (% of WT)
Media Concentration (μM)
MG-132
PS I
PS IV
Tyropeptin A
0
24
48
72
96 h
Proteasome inhibitors administered
Assay GC activity
B.
Relative L444P GC Activity
Lactacystin Media Concentration (μM)

Figure S4

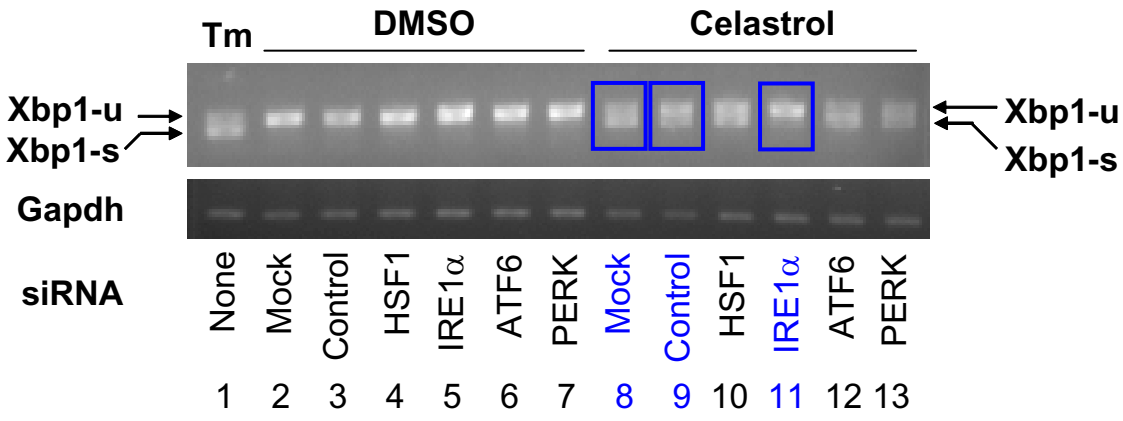
Tm
DMSO
Celastrol
Xbp1-u
Xbp1-s
Xbp1-u
Xbp1-s
Gapdh
siRNA
None
Mock
Control
HSF1
IRE1α
ATF6
PERK
Mock
Control
HSF1
IRE1α
ATF6
PERK
1 2 3 4 5 6 7 8 9 10 11 12 13

Figure S5

A.

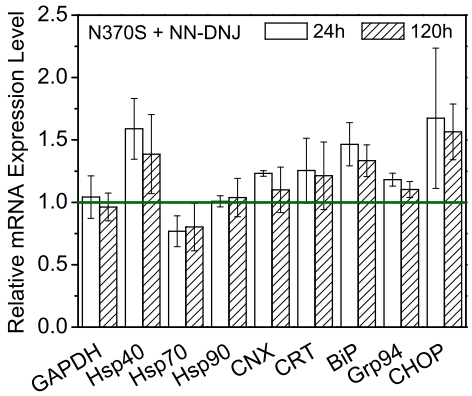

B.

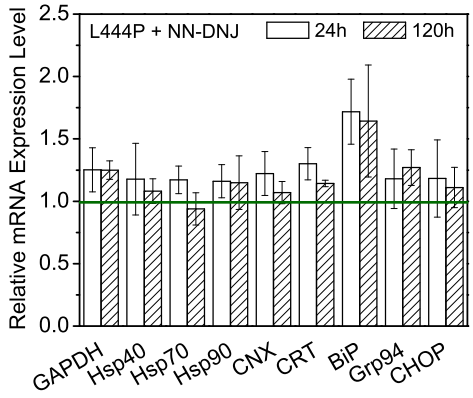

C.

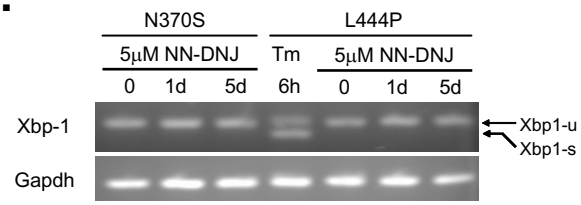

Figure S6

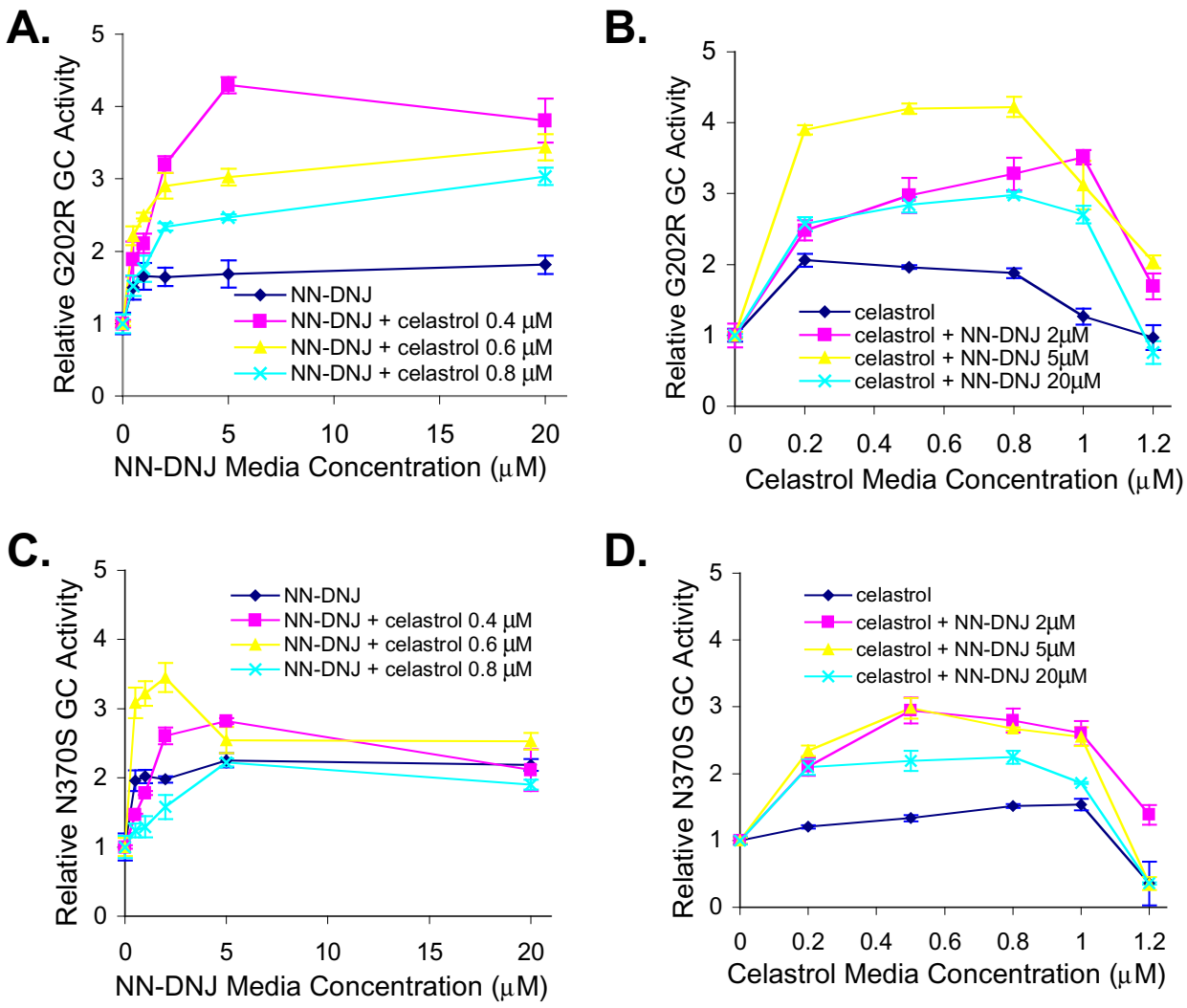
A.
Relative G202R GC Activity
NN-DNJ Media Concentration (μM)
NN-DNJ
NN-DNJ + celastrol 0.4 μM
NN-DNJ + celastrol 0.6 μM
NN-DNJ + celastrol 0.8 μM
B.
Relative G202R GC Activity
Celastrol Media Concentration (μM)
celastrol
celastrol + NN-DNJ 2μM
celastrol + NN-DNJ 5μM
celastrol + NN-DNJ 20μM
C.
Relative N370S GC Activity
NN-DNJ Media Concentration (μM)
NN-DNJ
NN-DNJ + celastrol 0.4 μM
NN-DNJ + celastrol 0.6 μM
NN-DNJ + celastrol 0.8 μM
D.
Relative N370S GC Activity
Celastrol Media Concentration (μM)
celastrol
celastrol + NN-DNJ 2μM
celastrol + NN-DNJ 5μM
celastrol + NN-DNJ 20μM

Figure S7

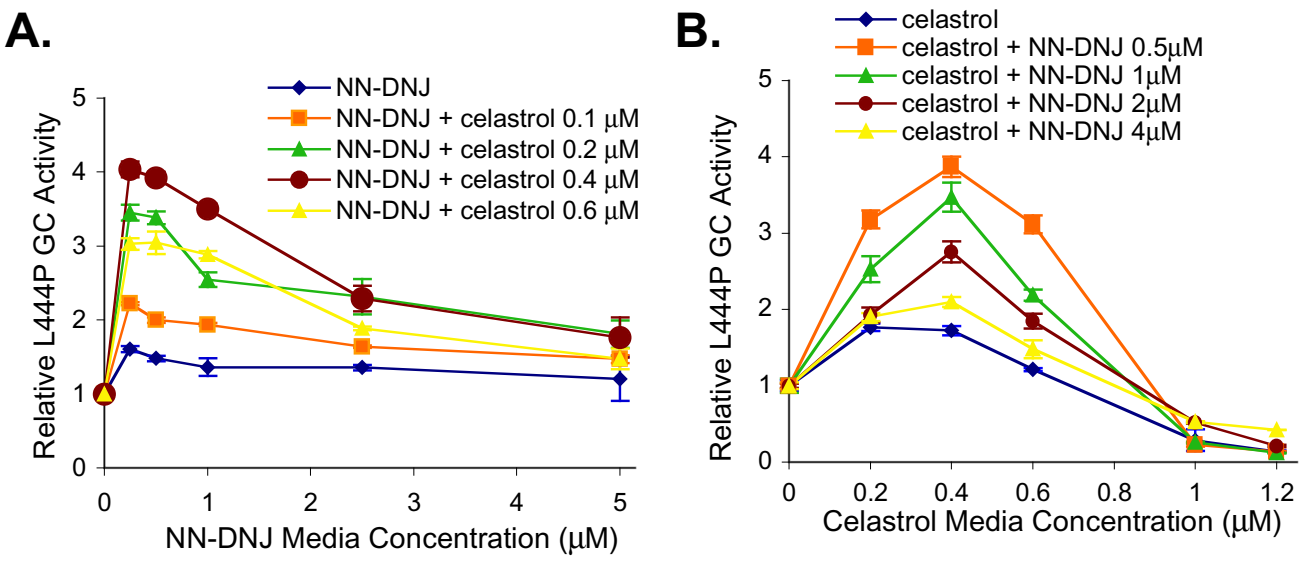
A.
NN-DNJ
NN-DNJ + celastrol 0.1 µM
NN-DNJ + celastrol 0.2 µM
NN-DNJ + celastrol 0.4 µM
NN-DNJ + celastrol 0.6 µM
Relative L444P GC Activity
NN-DNJ Media Concentration (µM)
B.
celastrol
celastrol + NN-DNJ 0.5µM
celastrol + NN-DNJ 1µM
celastrol + NN-DNJ 2µM
celastrol + NN-DNJ 4µM
Relative L444P GC Activity
Celastrol Media Concentration (µM)

Figure S8

A.

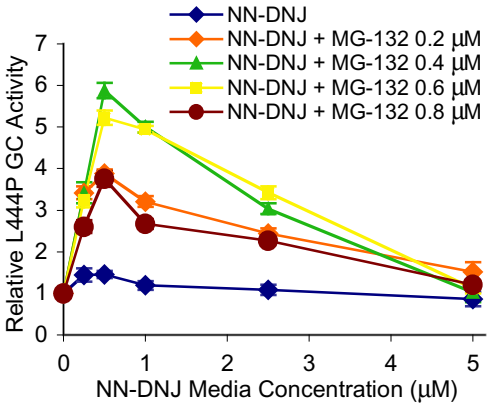
NN-DNJ
NN-DNJ + MG-132 0.2 µM
NN-DNJ + MG-132 0.4 µM
NN-DNJ + MG-132 0.6 µM
NN-DNJ + MG-132 0.8 µM
Relative L444P GC Activity
NN-DNJ Media Concentration (µM)

B.

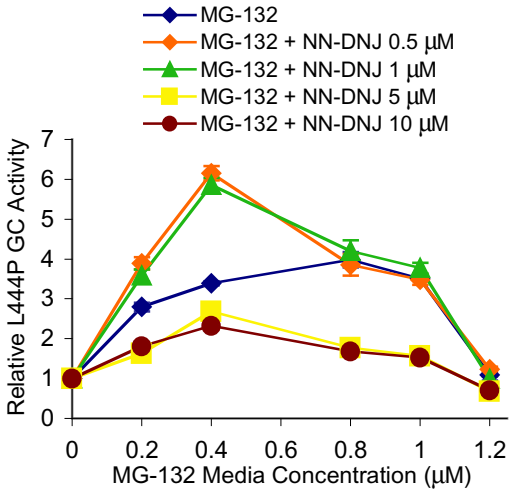
MG-132
MG-132 + NN-DNJ 0.5 µM
MG-132 + NN-DNJ 1 µM
MG-132 + NN-DNJ 5 µM
MG-132 + NN-DNJ 10 µM
Relative L444P GC Activity
MG-132 Media Concentration (µM)

Figure S9

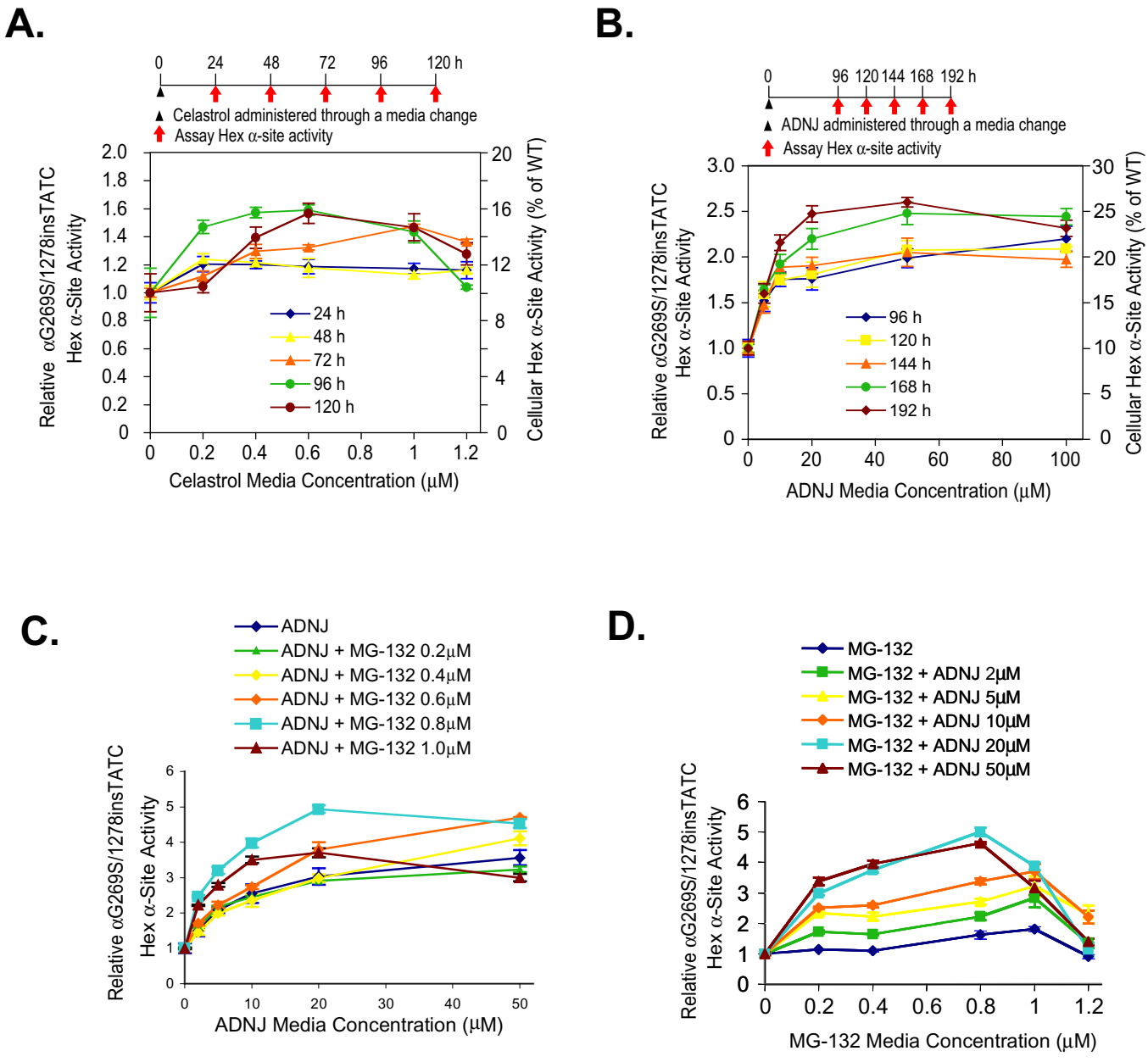
A.
0 24 48 72 96 120 h
Celastrol administered through a media change
Assay Hex α-site activity
Relative αG269S/1278insTATC Hex α-Site Activity
Cellular Hex α-Site Activity (% of WT)
24 h
48 h
72 h
96 h
120 h
Celastrol Media Concentration (μM)
B.
0 96 120 144 168 192 h
ADNJ administered through a media change
Assay Hex α-site activity
Relative αG269S/1278insTATC Hex α-Site Activity
Cellular Hex α-Site Activity (% of WT)
96 h
120 h
144 h
168 h
192 h
ADNJ Media Concentration (μM)
C.
ADNJ
ADNJ + MG-132 0.2μM
ADNJ + MG-132 0.4μM
ADNJ + MG-132 0.6μM
ADNJ + MG-132 0.8μM
ADNJ + MG-132 1.0μM
Relative αG269S/1278insTATC Hex α-Site Activity
ADNJ Media Concentration (μM)
D.
MG-132
MG-132 + ADNJ 2μM
MG-132 + ADNJ 5μM
MG-132 + ADNJ 10μM
MG-132 + ADNJ 20μM
MG-132 + ADNJ 50μM
Relative αG269S/1278insTATC Hex α-Site Activity
MG-132 Media Concentration (μM)

Figure S10

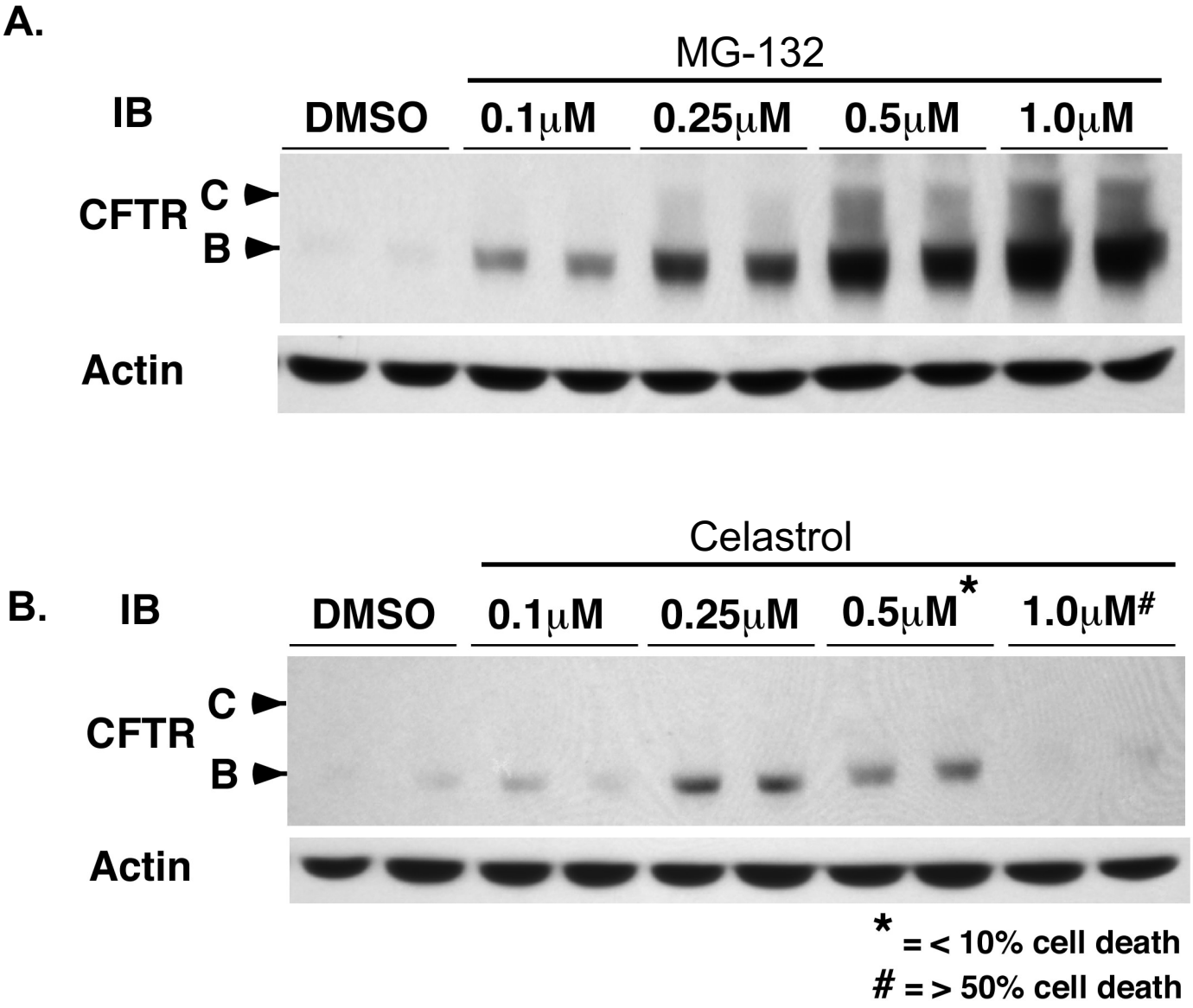
A.
MG-132
IB
DMSO
0.1μM
0.25μM
0.5μM
1.0μM
CFTR
C
B
Actin
Celastrol
B.
IB
DMSO
0.1μM
0.25μM
0.5μM*
1.0μM#
CFTR
C
B
Actin
* = < 10% cell death
# = > 50% cell death

Figure S11